1-1-2010

Enabling coherent superpositions of iso-frequency optical states in multimode fibers

Ofer Shapira

Ayman F. Abouraddy
University of Central Florida

Qichao Hu

Dana Shemuly

John D. Joannopoulos

See next page for additional authors

Enabling coherent superpositions of iso-frequency optical states in multimode fibers

Ofer Shapira,[1] Ayman F. Abouraddy,[2] Qichao Hu,[1] Dana Shemuly,[1] John D. Joannopoulos,[1] and Yoel Fink[1,*]

[1]*Research Laboratory of Electronics, Massachusetts Institute of Technology, 77 Massachusetts Avenue, Cambridge, MA 02329-0407USA*

[2]*The College of Optics & Photonics, University of Central Florida, 4000 Central Florida Blvd., Orlando, FL 32816 USA*

[*]*yoel@mit.edu*

Abstract: The ability to precisely and selectively excite superpositions of specific fiber eigenmodes allows one in principle to control the three dimensional field distribution along the length of a fiber. Here we demonstrate the dynamic synthesis and controlled transmission of vectorial eigenstates in a hollow core cylindrical photonic bandgap fiber, including a coherent superposition of two different angular momentum states. The results are verified using a modal decomposition algorithm that yields the unique complex superposition coefficients of the eigenstate space.

OCIS codes: (060.5295) Photonic crystal fibers; (060.2270) Fiber characterization

References and links

1. M. Skorobogatiy, C. Anastassiou, S. G. Johnson, O. Weisberg, T. D. Engeness, S. A. Jacobs, R. U. Ahmad, and Y. Fink, "Quantitative characterization of higher-order mode converters in weakly multimoded fibers," Opt. Express **11**(22), 2838–2847 (2003).
2. K. S. Lee, and T. Erdogan, "Fiber mode conversion with tilted gratings in an optical fiber," J. Opt. Soc. Am. A **18**(5), 1176–1185 (2001).
3. S. Ramachandran, P. Kristensen, and M. F. Yan, "Generation and propagation of radially polarized beams in optical fibers," Opt. Lett. **34**(16), 2525–2527 (2009).
4. Y. Yirmiyahu, A. Niv, G. Biener, V. Kleiner, and E. Hasman, "Excitation of a single hollow waveguide mode using inhomogeneous anisotropic subwavelength structures," Opt. Express **15**(20), 13404–13414 (2007).
5. A. F. Abouraddy, Q. Hu, O. Shapira, J. Viens, J. D. Joannopoulos, and Y. Fink, "Transmission of different angular-momentum modes in cylindrically symmetric photonic bandgap fibers in the near infrared," CLEO 2007.
6. T. G. Euser, G. Whyte, M. Scharrer, J. S. Y. Chen, A. Abdolvand, J. Nold, C. F. Kaminski, and P. St. J. Russell, "Dynamic control of higher-order modes in hollow-core photonic crystal fibers," Opt. Express **16**(22), 17972–17981 (2008).
7. S. Ghosh, J. E. Sharping, D. G. Ouzounov, and A. L. Gaeta, "Resonant optical interactions with molecules confined in photonic band-gap fibers," Phys. Rev. Lett. **94**(9), 093902 (2005).
8. D. G. Ouzounov, F. R. Ahmad, D. Müller, N. Venkataraman, M. T. Gallagher, M. G. Thomas, J. Silcox, K. W. Koch, and A. L. Gaeta, "Generation of megawatt optical solitons in hollow-core photonic band-gap fibers," Science **301**(5640), 1702–1704 (2003).
9. F. Benabid, J. C. Knight, G. Antonopoulos, and P. St. J. Russell, "Stimulated Raman scattering in hydrogen-filled hollow-core photonic crystal fiber," Science **298**(5592), 399–402 (2002).
10. F. Benabid, J. C. Knight, and P. St. J. Russell, "Particle levitation and guidance in hollow-core photonic crystal fiber," Opt. Express **10**(21), 1195–1203 (2002).
11. M. Bajcsy, S. Hofferberth, V. Balic, T. Peyronel, M. Hafezi, A. S. Zibrov, V. Vuletic, and M. D. Lukin, "Efficient all-optical switching using slow light within a hollow fiber," Phys. Rev. Lett. **102**(20), 203902 (2009).
12. P. Londero, V. Venkataraman, A. R. Bhagwat, A. D. Slepkov, and A. L. Gaeta, "Ultralow-power four-wave mixing with Rb in a hollow-core photonic band-gap fiber," Phys. Rev. Lett. **103**(4), 043602 (2009).
13. M. Greiner, O. Mandel, T. Esslinger, T. W. Hänsch, and I. Bloch, "Quantum phase transition from a superfluid to a Mott insulator in a gas of ultracold atoms," Nature **415**(6867), 39–44 (2002).
14. D. G. Grier, "A revolution in optical manipulation," Nature **424**(6950), 810–816 (2003).
15. B. Temelkuran, S. D. Hart, G. Benoit, J. D. Joannopoulos, and Y. Fink, "Wavelength-scalable hollow optical fibres with large photonic band gaps for CO2 laser transmission," Nature **420**(6916), 650–653 (2002).
16. K. Kuriki, O. Shapira, S. D. Hart, G. Benoit, Y. Kuriki, J. F. Viens, M. Bayindir, J. D. Joannopoulos, and Y. Fink, "Hollow multilayer photonic bandgap fibers for NIR applications," Opt. Express **12**(8), 1510–1517 (2004).

#119781 - $15.00 USD Received 6 Jan 2010; revised 6 Mar 2010; accepted 16 Mar 2010; published 28 May 2010

17. O. Shapira, K. Kuriki, N. D. Orf, A. F. Abouraddy, G. Benoit, J. F. Viens, A. Rodriguez, M. Ibanescu, J. D. Joannopoulos, Y. Fink, and M. M. Brewster, "Surface-emitting fiber lasers," Opt. Express **14**(9), 3929–3935 (2006).
18. S. Johnson, M. Ibanescu, M. Skorobogatiy, O. Weisberg, T. Engeness, M. Soljacic, S. Jacobs, J. D. Joannopoulos, and Y. Fink, "Low-loss asymptotically single-mode propagation in large-core OmniGuide fibers," Opt. Express **9**(13), 748–779 (2001).
19. D. John, Joannopoulos, Steven G. Johnson, Joshua N. Winn, and Robert D. Meade, "*Photonic Crystals,"* (Princeton University Press 2008).
20. O. Shapira, A. F. Abouraddy, J. D. Joannopoulos, and Y. Fink, "Complete modal decomposition for optical waveguides," Phys. Rev. Lett. **94**(14), 143902 (2005).
21. T. Engeness, M. Ibanescu, S. Johnson, O. Weisberg, M. Skorobogatiy, S. Jacobs, and Y. Fink, "Dispersion tailoring and compensation by modal interactions in OmniGuide fibers," Opt. Express **11**(10), 1175–1196 (2003).

1. Introduction

Waveguides supporting a multiplicity of iso-frequency states are characterized by an entropic increase in the population of states due to axially distributed perturbations. Initiating and maintaining a specific population through a controlled excitation and transmission of coherent superposition of eigenstates in a "constant entropy" regime can be highly desirable. The motivation is twofold. First, the formation of three dimensional field distributions can be achieved along the longitudinal dimension of a fiber providing a new medium for controlled light matter interactions. Second, the larger modal area and the controlled excitation could enable high-power lasers and waveguides to operate in higher energies without compromising the beam quality. Here we introduce an approach to synthesize, controllably transmit, and analyze coherent superpositions of fiber eigenmodes beyond the traditional single mode excitation. We show that in fact one may produce coherent linear superpositions of iso-frequency vectorial modes with different angular momenta and control their weights in real time.

In the past, coupling preferentially to a single specific fiber mode of weakly multimoded fibers has been achieved through the introduction of perturbations to the fiber structure such as fiber bends [1], gratings [2], or radial modulation to the refractive index profile [3]. Other approaches involve the modulation of the input beam phase or amplitude either by the fabrication of subwavelength polarization masks [4], or using a spatial light modulator (SLM) [5,6]. Nevertheless, to date, the controlled excitation and transmission of a coherent superposition of eigenstates has yet to be demonstrated. Indeed very little work has been done on the active use of controlled excitation of many-mode systems, predominantly due to the difficulty in synthesizing the required multi-mode profile, controlling its transmission, and the lack of a reliable approach to confirm the content of the propagated beam.

Controlling the eigenstate population of multimode waveguides enables the introduction of a characteristic axial length scale even in photonic structures that have complete axial translation symmetry. The length scale is associated with the spatial mode beating between non-degenerate iso-frequency modes and can be tailored by a proper choice of the expansion coefficients of the eigenstate superposition. The prospect of achieving such control offers a path towards studying physical phenomena that involve the interaction of a prescribed modulated field with the core matter over the extended length of the fiber. Indeed, the emergence of hollow core fibers in the past decade already pave the way to study the interactions of a tightly confined optical field with atoms, molecules, and particles over the extended length of the fiber [7–12]. Combined with the approach presented here, precise control of particles could be achieved, similar to optical lattices [13], and optical tweezers [14], but over the macroscopic length scale of a fibers. In this work we suggest a path to such realization by demonstrating a controlled population of several modes in a many-modes hollow core photonic bandgap (PBG) fiber. Figure 1 depicts a cross section of such fiber and an intensity pattern of a coherent superposition of four low-energy modes of such fiber demonstrating the ability to form periodic patterns inside the hollow core.

#119781 - $15.00 USD Received 6 Jan 2010; revised 6 Mar 2010; accepted 16 Mar 2010; published 28 May 2010

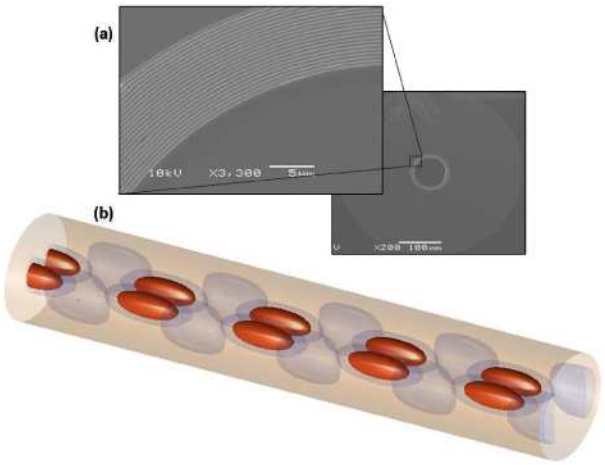

Fig. 1. (a) Scanning electron microscope micrographs of a multilayer cylindrically symmetric photonic band gap fiber cross section with a core diameter of 68 μm. (b) Three dimensional intensity distribution of a coherent superposition of four low energy eigenstates of the fiber. The red and blue regions correspond to surfaces in which the intensity drops to 1/4 and 1/16 of its maximal value, correspondingly.

2. Controlled eigenstates population in a PBG fiber

To demonstrate this approach, a cylindrically symmetric hollow-core photonic band gap fiber with core diameter of 68 μm was drawn using the preform-based fabrication method [15–17]. Such fiber supports several thousands of vectorial leaky-modes by confining light in the hollow core region via omnidirectional reflection from the cylindrically symmetric multilayer structure lining the core [18,19]. Figure 1 shows a cross sections of the fiber highlighting the multilayer structure of alternating polymer (polyethersulfone, 250-nm thick) and chalcogenide glass (As_2S_3, 145-nm thick).

The electric field of the nth mode of such structure is given by $\mathbf{\Psi}_n(\mathbf{r})\exp(-i\omega t) = \mathbf{R}_n(r)\exp[i(\beta_n z - \omega t + m\theta)]$ with three conserved quantities: the frequency ω, the axial wave vector β_n, and the angular momentum m. The total electric field can then be expressed by $\mathbf{\Psi}(\mathbf{r}) = \sum_n c_n \mathbf{\Psi}_n(\mathbf{r})$ where c_n are the complex expansion coefficients. In particular we study the superposition of two of the fundamental modes of this fiber by sculpting the phase profile of a Gaussian laser beam using a SLM and introducing it into the hollow-core fiber. Our choice of direct phase modulation, as opposed to holographic techniques, stems from the desire to avoid the computational latency associated with hologram calculations, allowing real time dynamic manipulation of the field. We verify that the desired superposition is achieved by using a modal decomposition technique that yields the complex expansion coefficients of the core-confined modes from intensity images of the fiber output [20]. The results of the modal decomposition confirm that we are in fact smoothly varying the relative weights of the two selected modes in a controlled manner. Note that, this technique is quite general and may be used in optical waveguides other than fibers and in any spectral range.

A common difficulty when dealing with many-mode waveguides is the inadvertent mode coupling that occurs along the fiber length due to perturbations to the fiber structure. While the exact coupling strength between two modes depends on the nature of the perturbation, in many practical cases, to a good approximation [18], the power that couples from one mode $\mathbf{\Psi}_n$ to another $\mathbf{\Psi}_{n'}$ is proportional to $\Delta\beta_{n',n}^{-2}$ where $\Delta\beta_{n',n}=\beta_n-\beta_{n'}$ is the mode separation. From general phase-space arguments it can be shown that the mode separation scales as $\Delta\beta \sim R^{-2}$ with R being the core radius. Using these general scaling arguments, the mode coupling

#119781 - $15.00 USD Received 6 Jan 2010; revised 6 Mar 2010; accepted 16 Mar 2010; published 28 May 2010

strength due to intentional perturbations such as fiber bends can be induced or inhibited by controlling the fiber bend radius. In the PBG fiber used here, with core diameter of roughly 45 wavelengths the fiber bend radius should be kept above 46 cm in order to inhibit any significant mode coupling. Mode coupling can also occur due to unintentional perturbations such as mechanical stress, microbends, or manufacturing imperfection. In such cases the strategy is to weaken the coupling strength by reducing the core diameter while assuring the fiber still supports the modes of interest.

For definiteness, we focus on two selected modes of this fiber, the TE_{01} and the HE_{11}. The intensity profile and polarization of the modes are shown in Fig. 2a. The TE_{01} with angular momentum zero is non-degenerate, purely transverse, with polarization vortex at the origin and doughnut shaped intensity profile. The HE_{11} is the lowest energy, double degenerate, hybrid mode with Gaussian like beam profile. We note that the $TE_{01,}$ the lowest-loss mode for such a fiber structure, is linearly polarized in $\hat{e}_\theta$, and has complete angular symmetry. Thus, unlike the usual doubly degenerate linearly polarized modes of a "single-mode" fiber, such a mode is truly single mode, and would thus avoid the usual pitfall of polarization mode dispersion [21]. The HE_{11} mode is linearly polarized (in Cartesian coordinates) and has angular momentum one. The transmission bandwidth of the HE_{11} is expected to be strongly affected by the narrower transverse magnetic (TM) band gap.

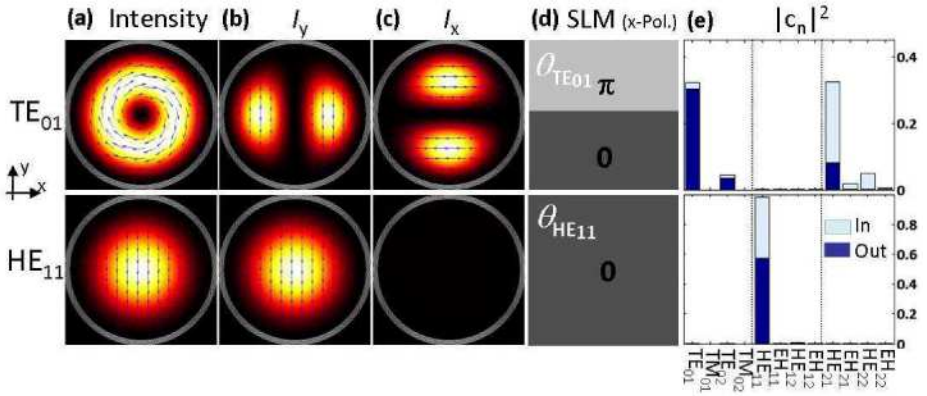

Fig. 2. (color). (a) Calculated intensity distributions of the TE_{01} (upper panel) and HE_{11} (lower panel) modes alongside their $\hat{y}$ **(b) and** $\hat{x}$ (c) polarizations. The SLM phase distributions (d) that are imparted to the $\hat{x}$-polarized Gaussian laser beam and the corresponding calculated coupling (e) to the twelve lowest modes with m<3 at the input (light blue) and after propagation through a meter long fiber (dark blue) taking into account differential modal losses.

One characteristic of these modes that is of importance in the discussion that follows is that each polarization component of the HE_{11} field has a constant phase, while the TE_{01} field has two halves that differ by π, parallel to the polarization of the linear projection (Fig. 2b-c). Since in general, modes supported by this fiber are vectorial, two orthogonal polarization components of the field need to be modulated in order to synthesize a perfect eigenstate. However, we note that modulation of a single polarization component using single SLM can result in preferential excitation owing to the differential modal losses of the PBG fiber [18]. The strategy to excite such low-energy modes can be therefore to modulate the phase distribution of the incident beam with the phase of one polarization component of the desired mode. The two phase distributions presented in Fig. 2d when imparted to a Gaussian beam profile result in nearly single mode propagation after a meter long fiber. Figure 2e provides theoretical calculation of the coupling coefficients at the input facet for each phase pattern (light blue) and at the output facet (dark blue) taking into account the propagation loss of each

#119781 - $15.00 USD Received 6 Jan 2010; revised 6 Mar 2010; accepted 16 Mar 2010; published 28 May 2010

mode. Thus, the simple control over the phase front, together with the fiber inherent mode filtering, suggests that one not only may controllably switch between these different modes but can also controllably excite superpositions of these modes.

3. Experimental setup and results

We used a linearly polarized laser beam at 1.5 μm from a tunable optical parametric oscillator (MIRA OPO, Coherent) that is synchronously pumped with a Ti:Sa laser (MIRA, Coherent) as our source. Figure 3a depicts the optical setup in which the linearly polarized Gaussian beam from our source is spatially filtered and magnified before it impinges normally on a reflective SLM (SLM PPM x7550, Hamamatsu) through a beam splitter. Then it reflects back to a lens (focal length 15 cm) that couples the beam to the fiber. The SLM imparts a computer-controlled phase distribution to the optical wave front. The beam at the output of the fiber is imaged using a microscope objective (x40) onto an InGaAs CCD camera (NIR SU320-1.7RT, Sensors Unlimited, Inc.).

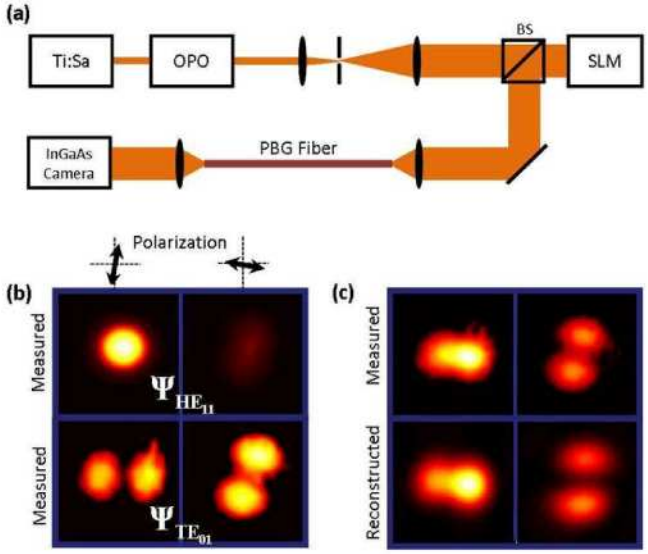

Fig. 3. (a) Schematic of the optical setup. (b) Measured intensity distribution for two perpendicular polarizations of the HE_{11} (upper panel) and TE_{01} (lower panel). (c) Far-field intensity patterns of the measured (upper panel) and reconstructed (lower panel) superposition of the two modes for a=0.625.

Applying the constant phase distribution, θ_{HE11}, to the SLM results in strong coupling to the HE_{11} mode as apparent from the measured near-field intensity images (upper panel of Fig. 3b) taken at two perpendicular polarizations by placing linear polarizer between the exit of the fiber and the camera. To preferentially excite the TE_{01} mode, θ_{TE01} is imparted to the beam. This overlaps with one Cartesian polarization of the TE_{01} and thus couples to it with maximum efficiency of 37% but also with the same efficiency to the HE_{21} (upper panel of Fig. 2e). However since the propagation length of the HE_{21} is shorter than of the TE_{01}, as indicated by Fig. 2e, the measured intensities after a meter long fiber indicates predominant TE_{01} component at the fiber output. Exact analysis of those measurements using mode decomposition technique is presented at the next section. 8. All measurements were performed at 1.5 μm wavelength, lying inside the fiber transmission photonic band gap. It is interesting to note that tuning the wavelength of the input field outside the TM band gap while staying inside the broader TE band gap results solely in the excitation of an extremely pure TE_{01} mode regardless of the input coupling condition. This can be understood by the fact that

#119781 - $15.00 USD Received 6 Jan 2010; revised 6 Mar 2010; accepted 16 Mar 2010; published 28 May 2010

even small residual coupling to TE mode survives the propagation through the fiber while other modes are not guided at all.

While it may be possible to identify some of the simpler low-order modes by using a linear polarizer to obtain intensity projection profiles, the same is not possible when the beam is a superposition of such modes. In such cases a distinct approach is required that reliably decomposes the output beam into its constituent modes revealing the relative (complex) contribution of each eigenmode, c_n. We previously developed a non-interferometric approach to achieve modal decomposition of the fields at the output of a general waveguide [20]. The technique utilizes a mapping of the two-dimensional field distribution onto the one-dimensional space of waveguide eigenmodes, together with a phase-retrieval algorithm to extract the amplitudes and phases of all the guided vectorial modes. This approach necessitates the acquisition of two near-field and two far-field intensity measurements at orthogonal polarizations. Here, near-field measurements were obtained by imaging the fiber facet to the camera using the microscope objective lens, while the far-field measurements were obtained by recording the output of the fiber with no lens. The size of the fiber core ensures that the diffracted field after a free-space propagation of one centimeter already corresponds to the far field.

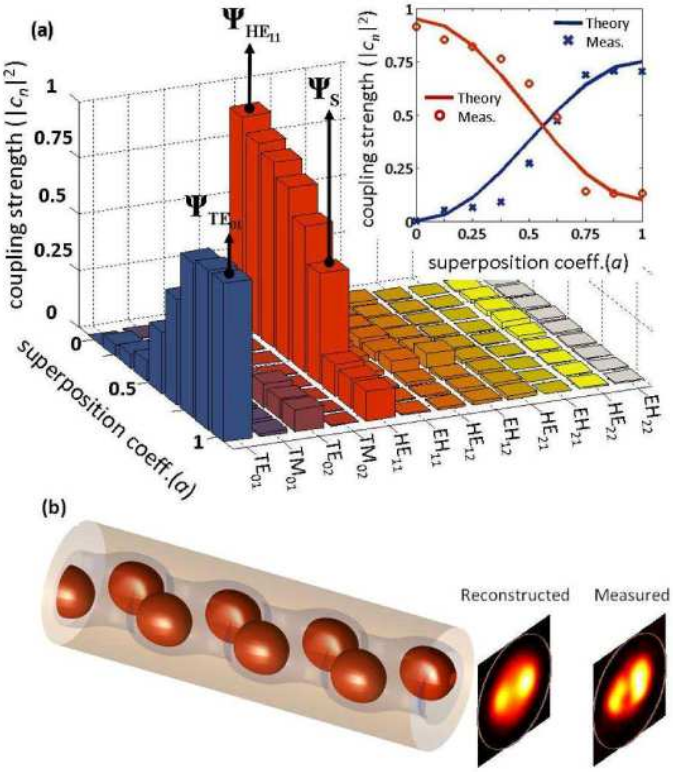

Fig. 4. (a) Coupling strength of the different modes as obtained from the mode decomposition algorithm for several values of the superposition coefficient a. The inset shows consolidated results for the main two modes together with theoretical calculation of the expected coupling coefficients. (b) Three-dimensional time averaged intensity pattern of the superposition defined by a = 0.625 (color scheme similar to Fig. 1) presented over 3.75 beat lengths ($2\pi\Delta\beta^{-1}$) of the two modes. To the right, the reconstructed and measured intensities at the end facet of the fiber are compared.

We have shown above that switching the phase distribution imparted to the beam from θ_{HE11} to θ_{TE01} results in the output beam switching between the HE_{11} and TE_{01} modes. It is

#119781 - $15.00 USD Received 6 Jan 2010; revised 6 Mar 2010; accepted 16 Mar 2010; published 28 May 2010

thus reasonable to expect that a weighted sum of the two phases will result in a beam which is composed of a weighted superposition of the two modes. More explicitly, in the limit where the two modes dominate the population of the output beam, by setting the SLM with the superposition phase $\theta_s = a \cdot \theta_{TE01} + (1-a) \cdot \theta_{HE11}$ where a is the superposition coefficient, the relative weight of the TE_{01} mode is expected to be $c_{TE01} = c_0 \exp[i\pi(1-a)/2]\cos[\pi(1-a)/2]$ where c_0 is the relative weight that corresponds to θ_{TE01} (a=1). We have implemented the above outlined idea experimentally by varying the phase of one half of the phase image from 0 to π while keeping the other half fixed to 0, corresponding to varying a from 0 to 1. For each value of a we acquired the four required intensity images. We applied the mode decomposition algorithm for each set and obtained the complex coefficients of the first 12 lowest energy modes with m<3. Examples of the acquired far-field intensity images for a = 0.625 are shown in Fig. 3c together with the intensity images of the reconstructed field. Neglecting modes with $|c_n|^2$<0.1, the coherent superposition as obtained from the mode decomposition algorithm is $\Psi_S = 0.69\, e^{i0.64} \Psi_{TE_{01}} + 0.7 \Psi_{HE_{11}}$. The absolute square of the coefficients for each value of a for all considered modes are shown graphically in Fig. 4a. As expected, the weight of the HE_{11} is maximal for a=0, and that of the TE_{01} is maximal for a = 1. For intermediate values a controlled superposition of the two eigenstates is obtained. The inset of Fig. 4a shows the relative weight of the TE_{01} and HE_{11} modes with the expected theoretical line obtained from the expression for c_{TE01}. The small discrepancies between the measurement and the theoretical values are attributed to the weak excitation of other modes that are neglected by the approximation made to the expression of c_{TE01}. The weak population of other modes at the output of the fiber is attributed to fast-decaying modes that are excited either by the input beam (as suggested by Fig. 2e) or inadvertently due to system imperfections. In the previously discussed case of a = 1 the relative weights of the measured modes as obtained from the decomposition (Fig. 4a) and the theoretical values (Fig. 2e) closely match for the TE_{01} and the TE_{02}, 0.72 and 0.1 respectively, while some discrepancies are observed for the HE_{11} and HE_{21}. The differences are attributed to possible misalignment of the input beam with respect to the fiber's core which can give rise to inadvertent excitation of modes as well as differential losses due to surface roughness at the core boundary interface.

This ability to control the eigenstates population provides a mean to determine and tailor the three dimensional field distribution along the fiber axis. Figure 4b shows the time averaged intensity distribution of $|\Psi_S|^2$ calculated for a longitudinal distance of several $\Delta\beta^{-1}$ until the end facet of the fiber where the measured and calculated cross section patterns are presented and compared. This result demonstrates the ability to construct a volumetric intensity (and field) patterns inside the fiber from knowledge of the complex expansion coefficients through control excitation of eigenstates at the input and verification of the modal content at the output of a waveguide. While this intriguing result is obtained by populating only two eigenstates in the superposition, scaling up to many modes can be achieved by the modulation of both polarization states. Since a single SLM allows the modulation of only one polarization component, the modal distributions that may be excited in the eigenstate space is limited to those that include modes with slower decay lengths than the superfluous modes that are excited due to the imperfect field structure at the input to the fiber. A complete control could be achieved by modulating both the phase and amplitude of the vectorial field by using an additional SLM or dividing the SLM pixel array to two regions treating each polarization separately.

4. Conclusions

We have demonstrated a simple approach to shape the field distribution inside a many-mode optical waveguide by a controlled population of its eigenstates. This modal control was verified by the use of a mode decomposition algorithm that uncovers the complex expansion

#119781 - $15.00 USD Received 6 Jan 2010; revised 6 Mar 2010; accepted 16 Mar 2010; published 28 May 2010

coefficients of the different modes in the output beam. The prospect of controlling the transmission properties of a multimode waveguide and molding the optical intensity distribution along the extended length of the fiber would provide new capabilities in the study of light guidance and light-matter interaction in waveguides.

Acknowledgments

This work was supported by ARO-ISN, DARPA and DOE. This project was also supported in part by the MRSEC program of the NSF. We also thank RLE for its support.

#119781 - $15.00 USD Received 6 Jan 2010; revised 6 Mar 2010; accepted 16 Mar 2010; published 28 May 2010